Proceedings World Geothermal Congress 2020+1
Reykjavik, Iceland, April - October 2021

Determination of Flow Connectivity and Heat Exchange Surface in Fractured Media Using Multicomponent Tracer Test

Xu Liang, Tianfu Xu, Bo Feng, and Zhenjiao Jiang

Key Laboratory of Groundwater Resources and Environment, Ministry of Education, Jilin University, Changchun, 130021, China

Liangxu2513@mails.jlu.edu.cn

Keywords: Multicomponent tracer test; Fractured media; Fluid connectivity; Heat exchange surface.

ABSTRACT

Multicomponent tracer tests are often used to understand advective and diffusive processes in fractured permeable media, and to determine the heat exchange capacity and spatial flow connectivity of fracture network. This study explored the behaviors of tracers, including chloride (inert tracer), lithium ion (sorptive tracer) and Rhodamine123 (thermally degrading tracer), in single-fracture column specimens under the temperature conditions of the hot dry rocks in the Gonghe Basin, China. It was found that adsorption ratio of Li^+ is in proportion to the concentration of rock powders representing the absorbent surface area. Both adsorption ratio of Li^+ and degradation ratio of Rhodamine123 increased with the temperature. The relative retardation of the sorptive and thermally degrading tracer concentration signals to the inert tracers was used to investigate the fluid/rock surface area and the temperature variation. The laboratory tests and analyses showed that application of multicomponent tracers proposed in this study can estimate the flow connectivity and monitor transient heat exchange capacity in fractured geothermal reservoirs.

1. INTRODUCTION

Geothermal resources offer tremendous potential as a renewable energy resource for the global energy security and increasing power demand. Heat resources stored in subsurface is commonly extracted by circulating fluid through injection and production doublet wells connected by the natural or artificial fracture networks. It is therefore of great importance to characterize and understand flow patterns in the fracture network before heat production. Many techniques have been employed to monitor the development of hydraulic fractures and to characterize the hydraulic connectivity of fracture networks, including electrical resistivity tomography (ERT), seismic imaging, distributed acoustic sensing (DAS), distributed temperature sensing (DTS) and tracer test (Siniscalchi A , et al., 2019). Among these techniques, tracer test has proven to be an effective method for identifying flow patterns, such as the structure of flow paths and preferential flow channels in fractured reservoirs (Karmakar S., et al., 2016). The quantitative interpretation of tracer tests can also provide an estimate of relevant transport parameters for the management and operation strategies of the geothermal systems (Axelsson, G., et al., 2001).

The use of tracers in geothermal applications was first suggested in model simulations by Los Alamos National Laboratory (LANL) during the Fenton Hill Hot Dry Rock geothermal project (Robinson et al., 1988). Because of the complexities involved in characterizing the flow and heat transport processes in geothermal reservoirs, multiple tracers of different physical and chemical characteristics have been explicitly considered. Chemically inert “conservative” tracers are commonly employed in groundwater tests, which are intended to flow passively through the subsurface without thermally degrading, chemically reacting, or adsorbing to rock surfaces. Conservative tracers can provide information about reservoir connectivities, fluid recharge location or direction and swept pore volumes.

To get further insight into the heat transfer process, cation-exchanging alkali metal tracers have been used for estimating fracture surface area based on the concept that their adsorption onto fracture surfaces by cation exchange should be proportional to the fracture surface area. The fracture surface area controls the rate of heat transfer between the host rock and the circulating injected water which affects the long-time performance of geothermal reservoirs. Reimus et al. (2003) conducted two cross-hole tracer tests involving the simultaneous injection of two inert solute tracers and lithium ion as sorbing solute tracer in two different intervals at a three-well complex and validated the applicability of a dual-porosity conceptual transport model in the saturated, fractured volcanic tuffs in the Yucca Mountain. In Sullivan et al. (2003), lithium sorption to volcanic tuff samples of varying composition was found to be positively correlated with surface area, although there were also correlations with mineralogy. Dean et al. (2015, 2018) carried out laboratory experiments to characterize cation-exchanging tracer behavior for fracture surface area with different temperature conditions. It was found that lithium cation exchange had a greater temperature dependence than cesium cation exchange. Reimus et al (2018) observed that lithium cation exchanged rapidly (attaining equilibrium within hours) and its transport behavior appeared to be dictated by cation exchange within a thin, low-porosity “rim zone” (< 0.05 mm) on rock surfaces that was accessed by diffusion. These studies all provide encouraging results for using lithium ion to interrogate fracture surface area for fractured geothermal systems.

The characterization and prediction of thermal drawdown and its spatial and temporal evolution is a major challenge in the context of geothermal reservoir management. It is also important for interpreting temperature anomalies to infer subsurface structures in the development of enhanced geothermal systems (Saar, 2011; Jung and Pruess, 2012).However, all currently available monitoring and characterization techniques, e.g., geophysical, borehole and/or tracer methods lack a direct in situ measurement for quantifying the thermal drawdown. The recently introduced thermo-sensitive tracers described by Nottebohm et al. (2010) have the potential to provide a new testing routine allowing the measurement of the thermal state of a geothermal reservoir. Peter and Scott (2014) demonstrated the successful application of Amino G in a tracer test at the Dixie Valley geothermal field. Maier et al., (2015a, 2015b) investigated the general behavior of phenol acetate (PhAc) in isothermal flow fields under various temperatures and flow rates. Schaffer et al. (2016) studied hydrolysis kinetics of carboxamides to extend the compound spectrum for hydrolyzable compounds as thermo-sensitive tracers for reservoir temperatures between 100 and 200°C. Qiu et al. (2016) investigated thermal stabilities of Rhodamine by thermogravimetric analysis (TG). This kind of fluorescent dye was proved to have the potential to provide a new testing tool allowing the measurement of the thermal state of a geothermal reservoir. Doro et al. (2015) and Shook et al. (2017)

developed methods with tracers and produced temperature to estimate the temperature conditions and the fracture volume and surface area swept of geothermal reservoirs.

The advantages of using multiple tracers with different physical and chemical characteristics to obtain transport parameter estimates have been clearly demonstrated (Małoszewski P et al., 1999; Serhat A and Abdullah G, 2018). Based on these previous efforts, we hypothesized that the differences between the breakthrough curves of cation-exchanging and thermally decay tracers and conservative tracers could potentially provide estimates of fracture surface area and temperature conditions in geothermal reservoirs. This study aims to investigate the effects of both local heat status and fracture surface on fractured media characteristics through multicomponent tracer experiments. Batch sorption experiments were performed to evaluate sportive cation interactions with rock particles and temperature-dependent kinetics of thermo-sensitivetracers. In this paper, we present the results of elevated temperature batch experiments and column transport experiments to further evaluate the method of using conservative, cation-exchanging and thermally decay tracers to interrogate flow connectivity and heat transfer properties in geothermal systems.

2. MATERIALS AND METHOD

2.1 Materials

2.1.1 Solid materials

The solid material (granite rock) used in the batch and column experiments was selected from the Gonghe-Guide Basin, Qinghai province where the first China EGS demonstration project will be built there. The hot dry granite was revealed with a highest temperature of 236ºC at the depth of 3705 meters at borehole GR1. Downhole temperature logs indicated that the geothermal gradient in the hot granite is 71.4ºC/km, with a mean heat flow of 119.3 mW/m^2 (Zheng et al., 2018). These granite samples were considered to be representative of the deep geothermal system in the Gonghe-Guide Basin. The granite rocks were crushed and sieved to a 1 mm particle size for batch experiments. The mineral composition of the sieved material was qualitatively determined by X-Ray Diffraction (XRD) (Table 1). The surface area of the sieved material was determined by a multipoint BET method with nitrogen as the sorbent.

Table 1: XRD-determined mineral fractions.

Mineral	Quartz	Alkali feldspar	Plagioclase	Calcite	Mica	Chlorite
Mineral mass fraction (%)	37	30	26	3	2	2

In column multi-tracer transport experiments, the granite rocks were processed into medium-sized cylinders with a diameter of 2.45 cm and length of 5-8 cm. Characterizing the flow-wetted surface and predicting thermal breakthrough in geothermal reservoirs dominated by sparsely spaced fractures is challenging. So the rock column was split into two halves in the middle through the Brazilian method to investigate flow patterns in an individual horizontal fracture. The surface area and roughness of the cut in the middle of rock columns were determined by the 3D scanning techniques.

2.1.2 Multicomponent tracer

The selection of tracers is a critical component in a successful tracer experiment. Using tracers with appropriate properties can help identify dominant transport mechanisms. Ideally, conservative tracers should move at the same velocity as the water and should be chemically inert during the course of the tracer test. In this study chloride (Cl^-) was chosen as the conservative tracer which was proved to be environmentally benign and thermally stable. Rhodamine123 dye (rhod-123) and monovalent cation lithium (Li^+) were chosen as a thermally degrading tracer and a sorbing tracer, respectively. All three of these tracers meet the requirements of high solubility, acceptable analytical detection limits, and low background concentrations in specific environments. The synthetic tracer solution, consisting of 10 mg/L Rhodamine123 and 1832.4 mg/L lithium chloride (LiCl) dissolved in the deionized water, was used as the working fluid in batch sorption experiments.

2.2 Batch sorption experiment

The concentration attenuation of the sorbing tracer relative to the nonsorbing tracers suggested that diffusion occurred primarily into matrix pores and stagnant water within the fractures. The Kd values describing the sorption kinetics can be measured in laboratory batch sorption tests using crushed rocks (Reimus, et al., 2003). Batch sorption experiments were conducted in triplicate in 50-ml Pyrex tubes. 0-15 g of the crushed and sieved granite material, was weighed into the tubes and equilibrated with working fluid with different reaction times. The liquid volume in each case was approximately 30 ml, yielding a solution to solid ratio of 0-0.5 g/ml. Li cation-exchange capacity (CEC) was determined for the solid materials by measuring the displacement of cations in a 1 molar Li solution. Reactive tracers can be used to observe the surface area of geothermal systems, because the reactive tracer interacts with the ambient rock causing retardation relative to a conservative tracer. This interaction is mainly dependent on temperature (Kuo et al., 2018). Moreover, to investigate the thermal stability of Rhodamine123, the batch experiments were carried out with different temperatures of 25 to 110℃. The batch sorption experiment scheme was summarized in Table 2. Aliquots of the supernatants after each sequential addition were analyzed for Li^+ by atomic absorption spectrometry and Rhodamine123 by fluorescence spectroscopy.

Table 2: Batch sorption experiment scheme.

Solution to solid ratio (g/ml)	Temperature (℃)	Time (min)
0		
0.1	25	
0.2	90	45-1200
1/3	110	
0.5		

2.3 Column transport experiments

Multi-tracer transport experiments were conducted in a high-pressure, high-temperature flow-through system that was designed to simulate geothermal reservoir conditions (Fig. 1). This system mainly consists of permeating pressure, temperature control, confining pressure, specimen holder, and data acquisition subsystem. A stainless steel specimen holder (approximate volume of 200 ml) was filled with the granite cylinder and sealed. The rock column was saturated by applying a vacuum at the outlet side of the vessel and then introducing deionized water into the vessel. The vessel was pressurized to 4.5 Megapascal (MPa), slowly heated to 110°C (pressure was maintained above the boiling point of the aqueous phase during heating) and allowed to equilibrate with deionized water at a constant flow rate of 3 ml/min for several hours. The confining pressure was maintained 1 MPa higher than the fluid pressure, to prevent water from flowing through the gap between the rock column and the holder.

The synthetic tracer solution, referred in Section 2.1.2, was loaded into a sample loop attached to a valve that allowed approximately 4 ml of tracer to be pulse-injected into the system without flow interruption. Immediately after injection, samples were continuously collected at downstream with 30-ml brown Pyrex tubes. These samples were collected in about 10 min each, capped, labeled with the sampling time. Aqueous samples collected from the column reactor in all experiments were analyzed for Rhodamine123 by fluorescence spectroscopy, Li^+ by atomic absorption spectrometry and Cl^- by potentiometric titration. The duration of the tracer experiments was approximately 8 hours depending on flow rate and tracer breakthrough. The data acquisition subsystem collects and records the flow velocity, permeating pressure, confining pressure, column temperature during the experiment.

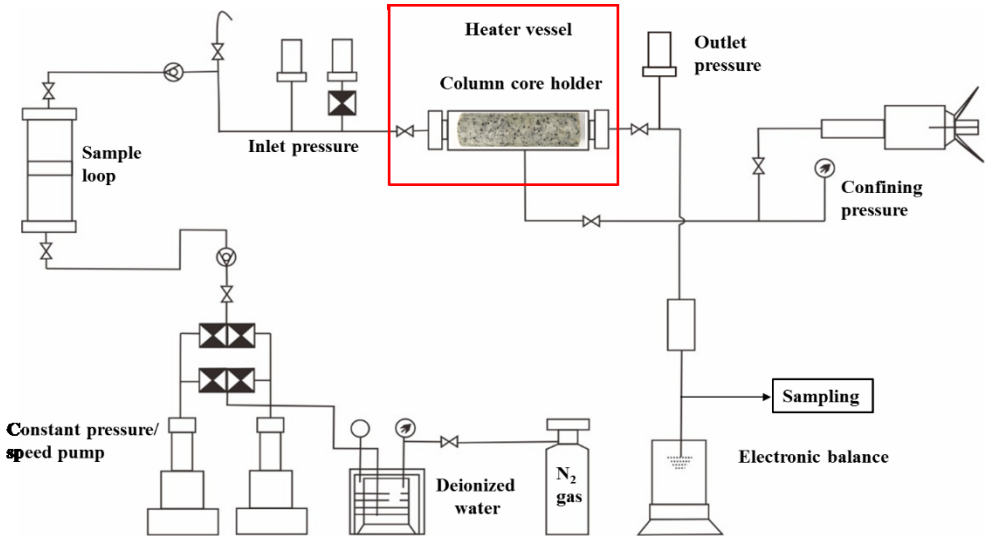

Figure 1: A schematic of the column transport experimental apparatus.

2.4 Mathematical Model

Some field-scale tracer tests demonstrated more than one tracer concentration peaks, e.g. Małoszewski et al, (2006), which indicates that the tracers may transport through cells along several different flow-paths characterized by different transit times and dispersivities. Małoszewski et al. (1992) first presented the relevant flow model for this assumption to describe tracer transport in a karst system. The multi-flow dispersion model (MFDM) assumes that the tracer transport through the cell can be approximated by a parallel combination of 1-D dispersion-convection Eq. 1. Each flow-path is characterized by a specific volumetric flow rate, mean transit time of water and apparent dispersivity. It is assumed that there are no interactions between the flow paths and that the mass of injected tracer is divided into several flow paths proportionally to the volumetric flow rates. The transport of an ideal tracer along the ith flow path is described by the 1-D dispersion-convection equation:

$$\frac{\partial C_i}{\partial t} - v_i \frac{\partial C_i}{\partial x} - \alpha_{Li} v_i \frac{\partial^2 C_i}{\partial x^2} = 0 \tag{1}$$

where $C_i(t)$ is the tracer concentration in the effluent from the ith flow-path; α_{Li} and v_i are the longitudinal dispersivity and the mean water velocity for the ith flow-path, respectively; x is the length of the flow path and t is the time after injection.

The outflow tracer concentration $C(t)$ is the flux weighted mean concentration from all flow paths observed in the outflow:

$$\mathrm{c(t)} = \sum_{i=1}^{N} \frac{Q_i}{Q} C_i(t) = \sum_{i=1}^{N} \frac{M_i}{M} C_i(t) = \sum_{i=1}^{N} \frac{M_i}{M} C_i(t) \tag{2}$$

where Q_i, M_i, R_i and Q, M, R are the volumetric flow rate, the mass of tracer, tracer recovery transported along the ith flow-path and the total measured in the outflow, respectively.
The semi-infinite solution of Eq. 1 in the case of the steady state flow and an instantaneous injection given by Kreft and Zuber (1978) has the following form:

$$C_i(\mathrm{t}) = \frac{M_i}{\frac{2Qt}{x_i}\sqrt{\pi \alpha_{Li} v_i \mathrm{t}}} exp\left(\frac{-(x_i - v_i t)^2}{4\alpha_{Li} v_i t}\right) \tag{3}$$

3. RESULTS

3.1 Batch sorption experiment

Changes in Li and Rhodamine123 relative concentrations in the elevated temperature batch experiment are shown in Fig. 2. The thermal stability of the synthetic tracer solution was firstly investigated with a solution volume to solid ratio of 0 g/ml in a temperature set from 25 to 110ºC.In the Fig. 2a, the Rhodamine123 still stays stable when temperature increases to 90ºC. The equilibrium partitioning of lithium between the sieved granite at room temperature is shown in Fig. 2b. The relative concentration change of Li has poorly defined trends, which is consistent with weak sorption at low temperature conditions that is partially observed by Dean et al., (2015). The amount of Li partitioning to the sieved granite slightly decreased with time which can probably be attributed to the fact that the mineral assemblage was likely altered at elevated temperatures. Thus sorption experiments with the same duration of 4 hours at the temperature of 110ºC were further analyzed to determine the relationship of Li partitioning amount and the solution volume to solid ratio, representing the solution volume to rock surface area ratio. As shown in Fig. 2d, the greater cation exchange capacity values for the sieved granite are consistent with the increase in surface area. There is a linear relationship between the relative concentration change of Li and the solution volume to rock powder surface a ratio derived from the batch sorption experiment data:

$$\frac{\Delta C}{C_0} = 11.23\frac{S_A}{V} \tag{4}$$

where ΔC and C_0 are the change of the tracer and the initial tracer concentration(mg/L), respectively; S_A is the BET rock powder surface area (cm²); and V is the tracer and rock powder solution volume (ml).

When temperature increased to 110ºC, there is clearly difference in the relative concentration change of Rhodamine123 and lithium in Fig. 2c. The thermal decay rate of Rhodamine123 at the temperature of 110ºC was calculated according to its concentration evolution in Fig. 2c as follows:

$$\ln\left(\frac{C(t)}{C_0}\right) = -0.0017t \tag{5}$$

where t is the time of the thermal decay reaction (min).

The decay rate was much faster at the beginning because of the physic sorption between Rhodamine123 and rock powder. Therefore, further batch experiments are going to be carried out to diminish the effects of physic sorption and calculate the thermal decay rate of R hodamine123 at a larger range of temperature conditions.

These relationships derived from batch experiments can be applied to the column tracer transport experiments to further interrogate the flow-wetted fracture surface area and effective temperature conditions which are vital to the heat transfer process in geothermal reservoirs.

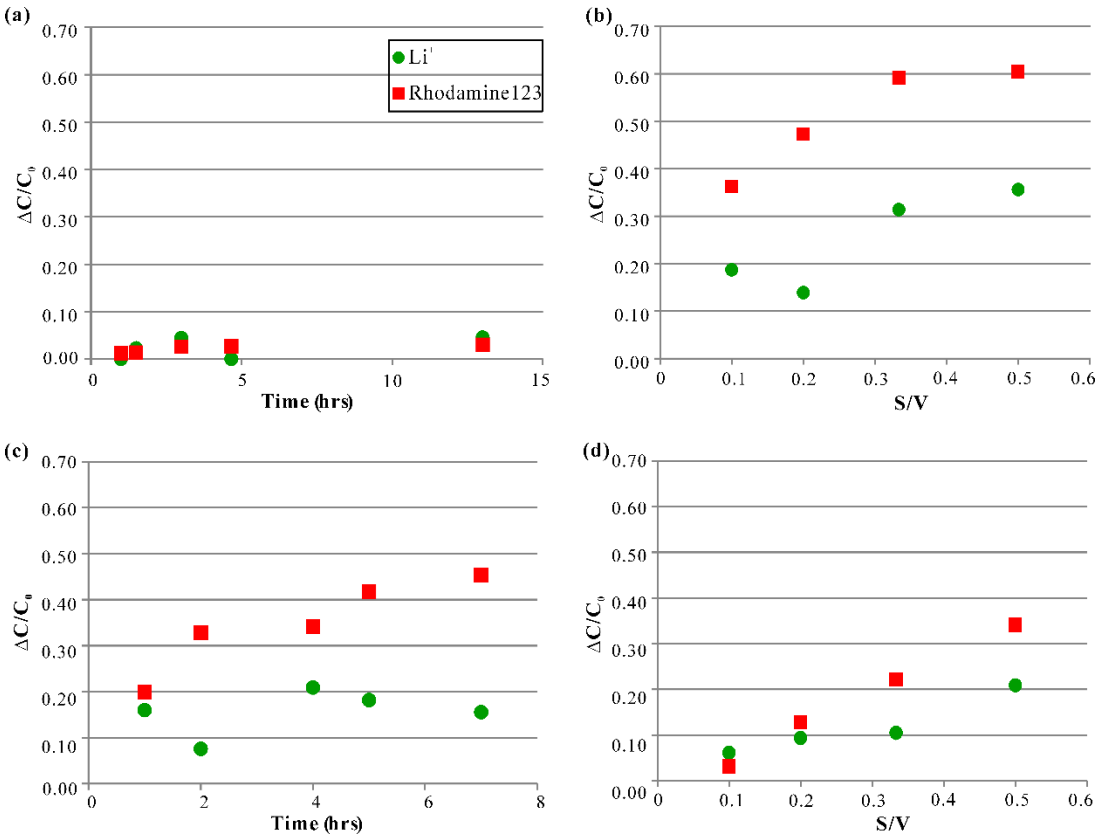

Figure 2: Relative concentration changes of tracers in batch sorption experiments: (a) Tracer solution volume to rock solid ratio=0, T=90ºC; (b) T=25ºC, t=13 hrs; (c) Rock powder to tracer solution ratio=0.5, T=110ºC; (d) T=110ºC, t=4 hrs.

3.2 Column tracer transport experiments

3.2.1 Conservative tracer experiment

In order to compare and verify the interpretation model referred in section 2.4, one group tracer transport experiment was first carried out with only conservative tracer, chloride (Cl^-). As described above, 4 ml sodium chloride (NaCl) solution with a high concentration of 80 g/L was pulse injected, then deionized was injected with a constant rate of 0.4 ml/min in this experiment. There was a pressure drop of 0. 36 Mpa maintained between the injection position and the outflow. The effluent solution was collected continuously and the chloride concentration was measured.

The interpretation of the tracer curve was possible with the MFDM as the fitting results shown in Fig. 3. The parameters of the MFDM are obtained by fitting Eq. 2, 3 to the tracer concentrations; these results are summarized in Table 3. The multi-step fitting procedure was applied to adjust model parameters to the measured tracer concentration evolution. The single flow path model (n=1) shows a good fitting to the concentration peak, but yields much lower tracer concentrations in the later part of the test as shown in Fig. 3 (a). Because it assumed only one flow path where convective flow dominated, the diffusive tracer was less than the other two models. The MFDM with two flow components (n=2) yields a preferential flow with a larger flow rate and a minimal longitude dispservity, and a general flow path taking the relative portion of more than 97% of the total flow according to the mass recovery rate in Table 3. Three flow components (n=3) indicated a much more uniform structure of the tested rock column with three flow path taking the relative portion of 21.49%, 44.44%, 34.07% of the total flow, respectively. The fitting parameters e.g. the longitude dispservity and the length of the flow path, in this case are contiguous to the parameters of the second general flow path obtained from the two flow components (n=2) model, which indicates that there is a less permeable flow path acting as a general channel for water and tracer in the fractured rock column. These results confirm earlier findings of Maloszewski and Zuber (1990) that matrix diffusion usually governs the transport of solutes in fractured rocks, whereas a proper representation of the fracture network is less important.

Table 3: Values of fitting parameters for conservative tracer test, obtained by applying the MFDM to the measured tracer-concentration data.

Flow patterns		Fitting parameters			
		M	v	α_L	x
		(mg)	(cm/min)	(cm)	(cm)
n=1		194.00	0.02	10.00	7.32
n=2	Flow path 1	5.65	0.58	0.75	9.19
	Flow path 2	187.11	0.15	49.50	48.93
n=3	Flow path 1	47.52	0.02	38.58	9.30
	Flow path 2	98.26	0.03	27.70	19.12
	Flow path 3	75.33	0.06	14.92	17.98

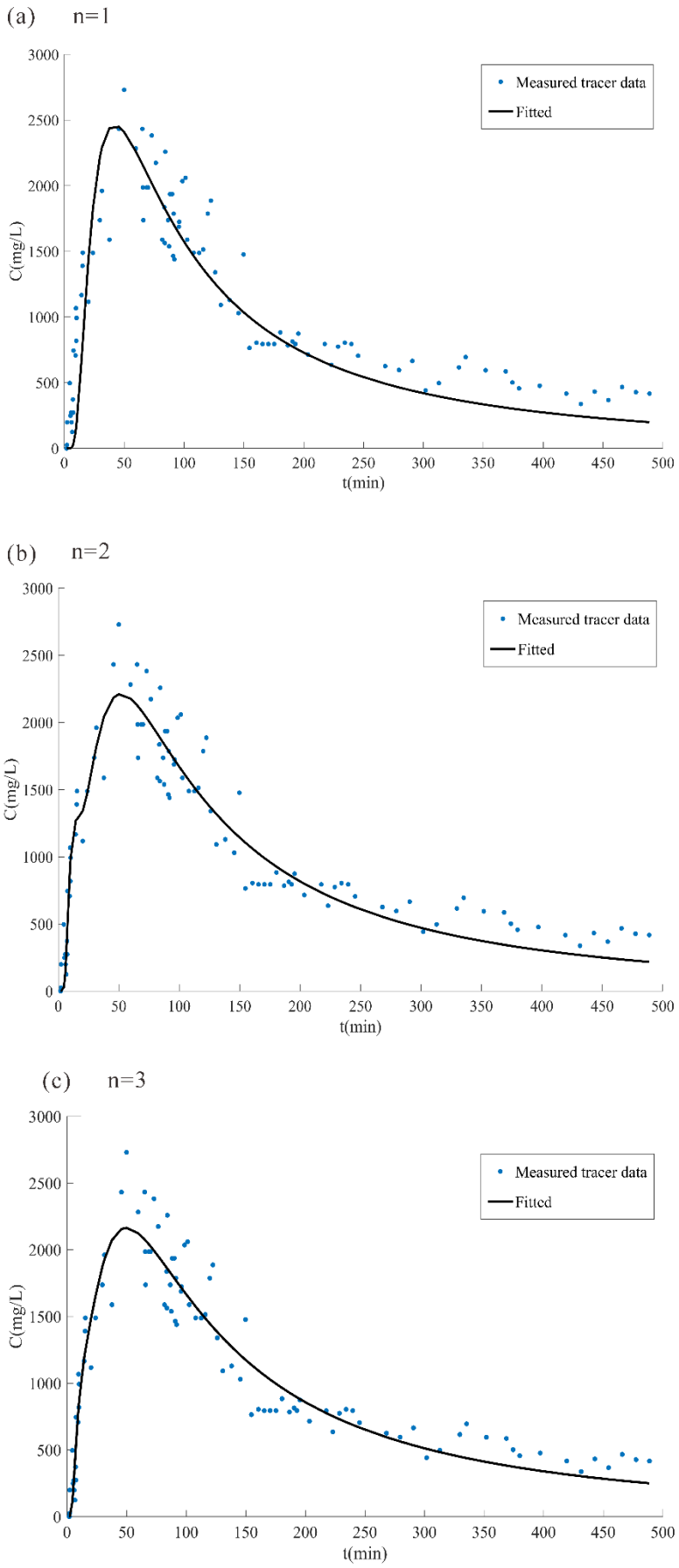

Figure 3: Measured chloride concentrations with time and the MFDM-fitted tracer concentration curve with (a) single flow path, (b) two flow paths and (c) three flow paths.

3.2.2 Multi-tracer experiment

The multi-tracer column transport experiment was carried out using a more intense condition with a constant injection rate of 3 ml/min. The tracer breakthrough curves from the multi-tracer column transport experiments are shown in Fig. 4. At the time of writing this paper, only one group of multi-tracer transport experiment has been analyzed for relative tracer concentration vs time. Results from early testing have been analyzed qualitatively for the arrival of the peak concentration that was quite unexpected with a generally dilution trend of the tracer breakthrough curve.

There is clearly difference in the transport of Rhodamine123 and chloride. Because of the thermal decay the concentration of Rhodamine123 decreased significantly and even lower than detection limit, resulting in a less mass recovery rate compared with chloride. Typically a sorbing tracer breakthrough arrival will be delayed as compared to a conservative tracer. Although the initial arrival time for the lithium was the same as the chloride tracer, the retardation became obvious after about 3 hours. The evolution for all the three tracers concentration was in a dilution trend and the retardation of reactive tracers became obvious in the later part of the experiment. This is probably owing to the fast flow rate and long sampling interval leading to the mixture of effluent with different trace concentrations.

Although the quantitatively analysis of the fracture surface area and effective temperature conditions are unavailable without the resident time of tracers in the rock column, the primary concentration evolution trend of tracers with different properties demonstrated in this study offers the potential method for further investigations to the flow and heat transfer mechanisms in heterogeneous fractured reservoirs.

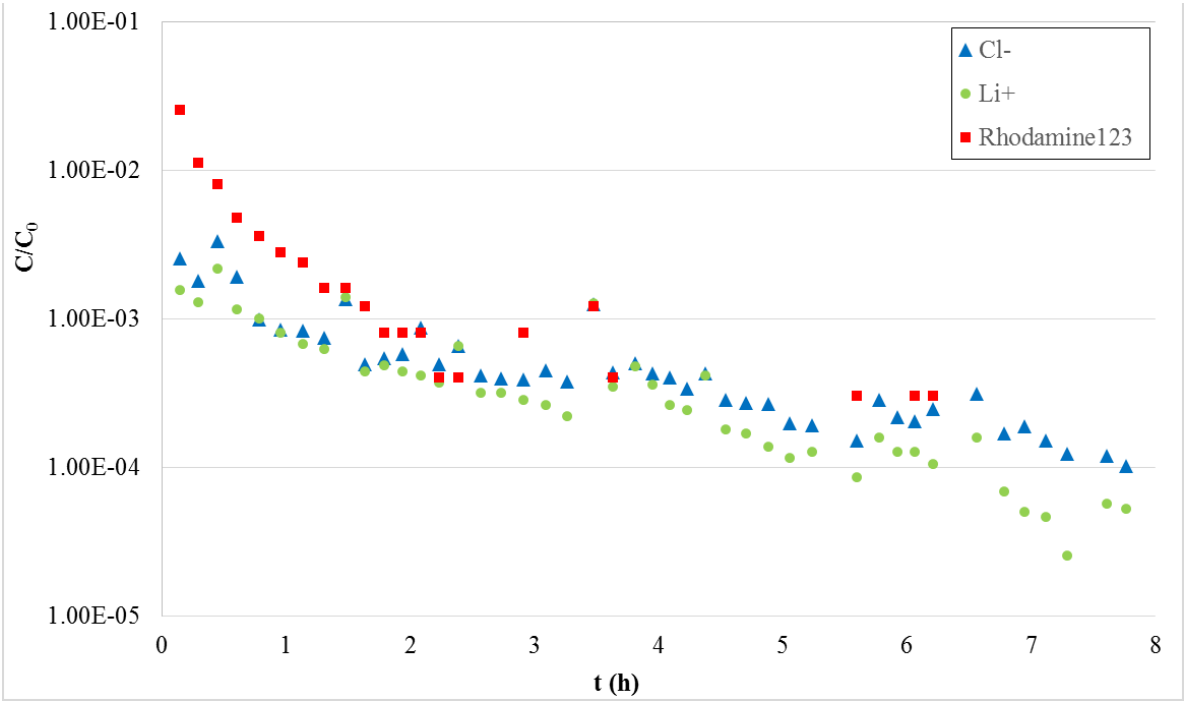

Figure 4: Breakthrough curves of Cl-, Li+ and Rhodamine 123 in the column transport experiment.

4. CONCLUSIONS

This study was not designed to test a hypothesis in a single-fractured medium, but to test multiple hypotheses in a real heterogeneous system. During this fracture characterization campaign, tracers of different physical and chemical characteristics have been simultaneously applied. Due to primary analysis of the batch sorption and column transport experiments, the adsorption and thermally decay behaviors of tracers can be preliminarily determined and experiment scheme can be further improved. The following conclusions can be drawn:

1. The adsorption and thermally decay behaviors of tracers can be determined by batch sorption experiments with a series of sieved rock at different temperature conditions to get proper tracer combination before the tracer transport tests.

2. The applicability of the multi-flow dispersion model to the interpretation of conservative tracer test in fractured rocks is demonstrated by contiguous values of parameters obtained from different models. These results confirm earlier findings of Małoszewski and Zuber (1990) that matrix diffusion acts as a main way for solutes transport in fractured rocks. The diffusion declines with a larger flow rate where convective flow dominates.

3. Rhodamine123 (adsorptive and thermally decay tracer) whose thermally-decay behavior is obvious when temperature is higher than 110°C, while its physic sorption behavior cannot be ignored. The potential of Rhodamine123 working as a thermal sensitive tracer to investigate temperature conditions in geothermal reservoir is going to be proved by additional experiments.

4. For lab-scale column tracer transport experiments, a higher concentration and less volume of injected tracer solution is more desirable to avoid early arrival of tracer concentration peak. The effluent solution should be better collected with a smaller volume and a shorter sampling interval for each sample to avoid the dilution.

ACKNOWLEDGMENTS

This work was jointly supported by the National Key Research and Development Program of China, Topic 3 (Grant No.2018YFB1501803), and by China Jilin Province Provincial School Joint Construction Project: New energy special (Grant No.SXGJSF2017-5).

REFERENCES

Axelsson, G., Flovenz, O.G., Hauksdottir, S., Hjartarson, A., Liu, J.: Analysis oftracer test data, and injection-induced cooling, in the Laugaland geothermalfield, N-Iceland, *Geothermics*, **30**, (2001), 697–725.

Dean C , Reimus P , Oates J , et al.: Laboratory experiments to characterize cation-exchanging tracer behavior for fracture surface area estimation at Newberry Crater, OR, *Geothermics*, **53**, (2015), 213-224.

Doro K O, Cirpka, Olaf A, Leven, Carsten.: Tracer Tomography: Design Concepts and Field Experiments Using Heat as a Tracer, *Ground Water*, **53(S1)**, (2015), 139-148.

Jung, Y., and K. Pruess.: A closed-form analytical solution for thermal single-well injection-withdrawal tests, *Water Resources Research*, **48**, (2012), p. 12.

Karmakar S , Ghergut J , Sauter M . Early-flowback tracer signals for fracture characterization in an EGS developed in deep crystalline and sedimentary formations: a parametric study, *Geothermics*, **63**, (2016), 242–252

Kuo, C.-H., S.-R. Song, P. Rose, and C.-M. Liu.: Reactive tracer experiments in a low temperature geothermal field, Yilan, Taiwan, *Geothermics*, **74**, (2018), 298-304.

Maier F , Schaffer M , Licha T.: Temperature determination using thermo-sensitive tracers: Experimental validation in an isothermal column heat exchanger, *Geothermics*, **53**, (2015a), 533-539.

Maier F , Schaffer M , Licha T.: Determination of temperatures and cooled fractions by means of hydrolyzable thermo-sensitive tracers, *Geothermics*, **58**, (2015b), 87-93.

Małoszewski P , Herrmann A , Zuber A.: Interpretation of tracer tests performed in fractured rock of the Lange Bramke basin, Germany. *Hydrogeology Journal*, **7(2)**, (1999), 209-218.

Małoszewski P , Zuber A.: Mathematical modeling of tracer behavior in short-term experiments in fissured rocks, *Water Resources Research*, **26(7)**, (1990),1517-0.

Małoszewski P, Wachniew P, Czupryński P.: Study of hydraulic parameters in heterogeneous gravel beds: Constructed wetland in Nowa Słupia (Poland), *Journal of Hydrology*, **331**, (2006), 630-642.

Nottebohm, M.,Licha,T.,Ghergut,I.,Nödler,K.,Sauter, M.: Development of thermo sensitive tracers for push-pull experiments in geothermal reservoir characterization, *Proceedings*, World Geothermal Congress 2010, Bali, Indonesia, (2010).

Peter R and Scott C.: The Use of Amino G as a Thermally Reactive Tracer for Geothermal Applications, *Proceedings*, 39th Workshop on Geothermal Reservoir Engineering, Stanford, California, (2014).

Qiu S , Chu H , Zou Y , et al.: Thermochemical studies of Rhodamine B and Rhodamine 6G by modulated differential scanning calorimetry and thermogravimetric analysis, *Journal of Thermal Analysis & Calorimetry*, **123(2)**, (2016), 1611-1618.

Reimus P, Dean C, Newell D.: Evaluation of a cation-exchanging tracer to interrogate fracture surface area in enhanced geothermal systems, *Geothermics*, **71**, (2018), 12-23.

Reimus P W , Haga M J , Adams A I , et al.: Testing and parameterizing a conceptual solute transport model in saturated fractured tuff using sorbing and nonsorbing tracers in cross-hole tracer tests, *Journal of Contaminant Hydrology*, **62(4)**, (2003), 613-636.

Robinson, B.A., Tester, J.W., Brown, L.F.: Reservoir sizing using inert and chemically reacting tracers, *SPE Form. Eval.* **3 (1)**, (1988), 227-234.

Saar M O.: Review: Geothermal heat as a tracer of large-scale groundwater flow and as a means to determine permeability fields, *Hydrogeology Journal*, **19(1)**, (2011), 31-52.

Schaffer M , Idzik K R , Wilke M , et al.: Amides as thermo-sensitive tracers for investigating the thermal state of geothermal reservoirs, *Geothermics*, **64**, (2016), 180-186.

Serhat A and Abdullah G.: Comprehensive Tracer Testing in the Germencik Field, *Proceedings*, 43rd Workshop on Geothermal Reservoir Engineering, Stanford, California, (2018).

Shook G M , Suzuki A . Use of tracers and temperature to estimate fracture surface area for EGS reservoirs, *Geothermics*, **67**, (2017), 40-47.

Siniscalchi A , Tripaldi S , Romano G , et al.: Reservoir Structure and Hydraulic Properties of the Campi Flegrei Geothermal System Inferred by Audiomagnetotelluric, Geochemical, and Seismicity Study, *Journal of Geophysical Research-Solid Earth* , **124**, (2019), 5336-5356.

Sullivan, E.J., Reimus, P.W., Counce, D.A.: Transport of a reactive tracer in saturated alluvium described using a three-component cation-exchange model, *Contam. Hydrol*. **62–63**, (2003), 675–694.

Zheng, Y.X., Shan W.J., Zhao C.L., Jiang R., and Li Y.N.: The Drilling Technology for the GR1 Well in Hot-Dry Rock of Gonghe, Qinghai Province, *Geology and Exploration*, **54**, (2018), 1038-1045.